AD-A090 396 ARMY MISSILE COMMAND REDSTONE ARSENAL ALABAMA F/G 21/2
THREE-DIMENSIONAL FINITE ELEMENT COMBUSTION INSTABILITY ANALYSIS
JUN 80 HACKETT, ROBERT M.

UNCLASSIFIED NL

1 OF 1
AD A090396

END
DATE
FILMED
11-80
DTIC

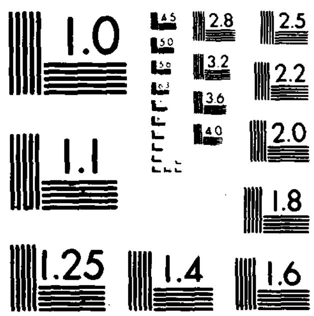


MICROCOPY RESOLUTION TEST CHART
NATIONAL BUREAU OF STANDARDS 1963 A

# THREE-DIMENSIONAL FINITE ELEMENT COMBUSTION INSTABILITY ANALYSIS

JUN 1980

ROBERT M. HACKETT, PhD
PROPULSION DIRECTORATE, US ~~ARMY MISSILE LABORATORY~~
REDSTONE ARSENAL, ALABAMA 35809

## INTRODUCTION

The phenomenon of oscillatory combustion instability in solid rocket motors results from the responsiveness of the combustion process to oscillations in the flow environment. Because of the high probability of combustion instability in low signature motors and the attendant jeopardy to successful motor and system performance, the capability of instability prediction is of unquestioned importance. The state-of-the-art in the field of linear analysis of combustion instability is based on a perturbation of the acoustic field in the burning propellant and an evaluation of the growth/decay coefficient associated with the acoustic pressure waves; a positive coefficient indicates an amplification of the waves and, therefore, instability, and a negative value implies attenuation of the waves and stability.

In early 1975 the development of a Standardized Stability Prediction Method for Solid Rocket Motors [1] was begun by Aerojet Solid Propulsion Company under contract with the Air Force. It was decided that this method would employ the NASTRAN finite element fluid analysis option which was developed for rocket acoustic cavity analysis [2,3,4,5]. The NASTRAN finite element analysis is axisymmetric and approximates the effect of radial slots (Figure 1) on the cavity acoustics. As long as the slot width is relatively narrow, the approximation provides an accurate model of the cavity acoustic response, but as the slot width increases, the accuracy diminishes. The NASTRAN option as used in the standardized method does not provide for the coupling of the vibratory response of the solid propellant grain to that of the acoustic cavity and hence does not provide a means of evaluating the damping of the acoustic oscilliations by the propellant grain response. An additional limiting feature of the standardized method is that it employs a post processor, separate from the other analyses, for evaluating the growth/decay coefficient.

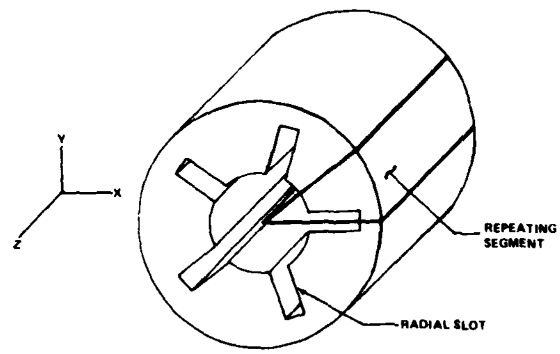


Figure 1. Three-dimensional cavity-solid propellant model.

The three-dimensional analysis package presented herein was developed primarily to provide 1) more generality, and therefore more accuracy in modeling complex cavity geometries, 2) a means of predicting the damping of acoustic oscillations by the solid propellant grain, 3) an integrated program designed solely for the purpose of combustion instability prediction with ease of use, and 4) a means of coupling the combustion instability analysis to an internal ballistics analysis. The developed package possesses all of these positive features as well as certain inherent, somewhat unappealing features associated with "bigness" which will be pointed out later in the paper.

The main aspects of the developed three-dimensional code are listed as follows and will be elaborated upon subsequently in the paper:

1) It utilizes a three-dimensional finite element mesh generator especially adapted to provide input to the program.

2) It utilizes the principle of dihedral symmetry which enables a consideration of only the smallest repeating geometrical segment.



149

3) It couples the response of the gas cavity with that of the solid propellant grain to enable the calculation of the frequency of the coupled system and the damping provided by the propellant grain.

4) It provides for modeling the propellant grain as a nearly incompressible material (which differs from the common minimum potential energy formulation).

5) It utilizes the principle of condensation, wherein, in this case, the fluid pressure degrees-of-freedom are designated "master" and the solid propellant displacement and mean pressure parameter degrees-of-freedom are designated "slave." This enables a major reduction in the size of the problem; the number of equations is reduced from the total number of degrees-of-freedom of the coupled system to the number of fluid pressure degrees-of-freedom.

6) It provides the option of considering the response of the gas cavity alone (which models the cavity boundaries as being "acoustically hard"). This option might be utilized in certain cases where a savings in computer costs or storage is a dominant consideration. In this case the condensation approach previously described obviously would not be taken.

7) It calculates the three-dimensional potential flow field.

8) It evaluates the stability integrals for the calculation of the net driving/damping coefficient for each mode.

## FINITE ELEMENT MESH GENERATION

It is only necessary to develop a finite element mesh for one repeating segment (Figure 1) of the total cavity-grain rocket geometry. This is true because of the employment of the principle of dihedral symmetry in the program. Although the three-dimensional element used in the program for both the cavity region and the propellant grain is a tetrahedron [6], the mesh is that of bricks, each brick, or quasi-hexahedron, being comprised of five basic tetrahedra. The breakdown of the quasi-hexahedra into tetrahedra is performed internally. The mesh generator is an efficient routine which automatically creates the complete finite element mesh, for both cavity and solid propellant regions, from a minimal amount of input. Each repeating segment is sectioned in the longitudinal or z-direction, with each section comprised of a number of quadrilateral parts which are identified by a counterclockwise listing of their part boundary curves.



147

Part boundary curves may be ellipses as well as straight lines and their points of intersection are designated by I,J indices as shown in Figure 2.

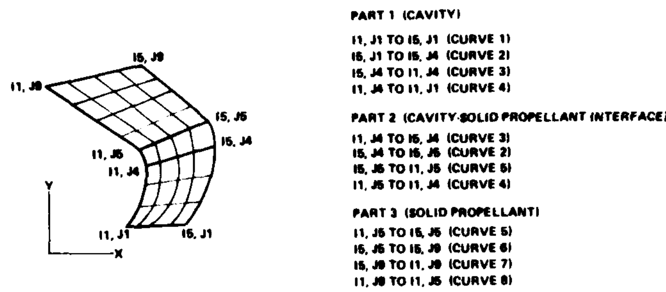


Figure 2. Finite element mesh definition for cavity-solid propellant.

By coupling the output of a standard internal ballistics analysis computer code with the mesh generator one can obtain a combustion instability analysis at any stage of performance, i.e., at any instant from ignition of the propellant to burnout. This has been done through the definition of additional part boundary curves, which conform to the geometry of the different zones of burning for the differing cavity-grain configurations. With the transfer of a small number of geometric parameters from the output of the internal ballistics code to the mesh generator, a complete combustion instability analysis can be initiated and automatically performed. The designation of these parameters and a detailed description of the development of the coupling program are found in References [7] and [8]. Presently the coupling of an internal ballistics analysis with the combustion instability analysis is limited to the consideration of axisymmetric and star cross-section geometries, but increased part boundary curve definition is a matter of expansion of the program, not of additional development.



(150)

## DIHEDRAL SYMMETRY

If a geometrically defined body is made up of identical segments symmetrically arranged with respect to an axis, the degrees-of-freedom for a finite element analysis can be transformed into uncoupled symmetrical components, thereby greatly reducing the number of equations which must be solved simultaneously [9]. A further reduction can be effected if each segment has a plane of reflective symmetry. Dihedral symmetry is the term applied to this latter condition. It can be seen from Figure 1 that a typical solid rocket geometry meets this requirement and, therefore, the principle of dihedral symmetry can be employed in a three-dimensional (cylindrical coordinate) analysis. The application of the principle to this problem is explained in detail in Reference [10] and will not be reproduced here, but the resulting analysis will be discussed.

Employing the principle of dihedral symmetry, the program computes three distinct types of acoustic harmonics: the zero harmonic, the K harmonics, and the N/2 harmonic. The zero harmonic exists for all cases. The number of possible K harmonics is given by

$$K = 1, \dots, L \tag{1}$$

where the harmonic index L is given by

$$L = \frac{N - 1}{2} \text{ (if N is an odd number)} \tag{2a}$$

$$= \frac{N - 2}{2} \text{ (if N is an even number)} \tag{2b}$$

where N is the number of radial slots or lobes. The N/2 harmonic exists only when N is even. Referring to the geometry of Figure 1, then, one could calculate the zero, first, and second harmonics, the latter two being K harmonics. The longitudinal modes associated with each harmonic are calculated as requested by the user. The result of this calculation (eigensolution) is the natural circular frequency associated with each acoustic mode and the corresponding acoustic pressure distribution (normalized acoustic pressure at each finite element nodal point) for the smallest repeating segment. The pressure distribution for each of the other segments is then simply calculated automatically through the dihedral transformation matrix. The acoustic velocity components (constant for the region occupied by each cavity tetrahedral element) are computed from the acoustic pressure nodal point values for those cavity elements which are adjacent to the propellant grain.



(151)

The theoretical formulation of the complete three-dimensional finite element analysis, in which the natural circular frequency, the acoustic pressure distribution, and the element acoustic velocities are calculated, is given in Reference [11] and will not be repeated here. Reference [12] also presents the theoretical finite element formulation which was used in the development of this program.

## COUPLED RESPONSE

The presence of the solid propellant grain can significantly shift the acoustic system frequency from that of the gas phase alone, a portion of the acoustic energy being dissipated by the deformable solid material. This effect can be one of the more significant sinks for acoustic energy in both large and small rocket motors, the amount of damping depending on the grain geometry and mechanical properties and on the acoustic mode shape and natural frequency.

In order to evaluate the coupled cavity-solid propellant grain response it is necessary to model, by the finite element method, both cavity and grain. This, of course, greatly increases the size of the problem to be solved, from the standpoint of number of initial degrees-of-freedom. The coupled finite element formulation of Reference [12], which is coded in the three-dimensional program, is expressed in matrix form by:

$$\left(\left[\begin{array}{c|c} F & 0 \\ \hline -U^T & K \end{array}\right] - \lambda^2 \left[\begin{array}{c|c} C & U \\ \hline 0 & \begin{array}{c|c} M & 0 \\ \hline 0 & 0 \end{array} \end{array}\right]\right)\left\{\begin{array}{c} p \\ \hline \Delta \\ \hline H \end{array}\right\} = 0 \qquad (3)$$

where [F] is the fluid inertia matrix, [C] is the fluid compressibility matrix, [K] is the solid stiffness matrix, [M] is the solid consistent mass matrix, [U] is the matrix which couples acoustic pressure degrees-of-freedom to solid displacement degrees-of-freedom, {p} is the acoustic pressure vector, {Δ} is the solid displacement vector, {H} is the mean pressure parameter vector (to be elaborated upon later), and $\lambda^2$ is the eigenvalue of the coupled system.

The structural damping can be attributed to the out-of-phase response of the solid propellant grain, which is measured in terms of the complex shearing modulus of the grain, which, in turn, results in a complex eigenvalue for the coupled system. The imaginary part of the complex eigenvalue obtained from the eigensolution is the natural circular frequency of the coupled system while the real part is the structural damping rate.

Since the complex shearing modulus is frequency dependent, a series of iterations may be necessary before the accurate value of complex modulus for input into the program is determined.

## PROPELLANT GRAIN MODELING

Since the propellant grain is only accurately modeled as a nearly incompressible material, the well-known standard Navier displacement formulation, in conjunction with the Ritz procedure, would lead to inaccuracies in the finite element modeling of the grain. In order to avoid this situation the solid finite element formulation utilized in this program is that of a linear displacement-linear mean pressure tetrahedron [13]. It is similar to the Herrmann variational formulation [14], which employs a linear displacement function and a constant mean pressure function. The finite element modeling of the propellant grain used in this program is outlined in detail in Reference [12] and will not be repeated here.

## EIGENVALUE ECONOMIZER - CONDENSATION

The extraction of eigenvalues and eigenvectors is a much more expensive operation than is the solution of simultaneous linear equations. It requires roughly twice as much time to extract a single eigenvalue as to do a single "static" analysis. In order to reduce or "condense" the number of degrees-of-freedom in the eigensolution, the following technique is utilized in the three-dimensional program. Further details of the method are found in Reference [15].

The original formulation of the coupled system is given by Equation 3, where the number of degrees-of-freedom is equal to the number of cavity nodal point pressures, plus the number of solid propellant nodal point displacement components, plus the number of solid propellant nodal point mean pressure parameter values (one at each propellant grain nodal point), for the analyzed repeating segment. The condensed formulation is given by:

$$\left( \begin{bmatrix} F_r \end{bmatrix} - \lambda^2 \begin{bmatrix} C_r \end{bmatrix} \right) \left\{ p \right\} = 0 \tag{4}$$

where

$$\begin{bmatrix} F_r \end{bmatrix} = \begin{bmatrix} I \\ \hline K^{-1}U^T \end{bmatrix}^T \left[ \begin{array}{c|c} F & 0 \\ \hline -U^T & K \end{array} \right] \begin{bmatrix} I \\ \hline K^{-1}U^T \end{bmatrix} \tag{5a}$$



153

and
$$\left[ C_r \right] = \left[ \begin{array}{c} I \\ \hline K^{-1}U^T \end{array} \right]^T \left[ \begin{array}{c|c} C & U \\ \hline 0 & \begin{array}{c|c} M & 0 \\ \hline 0 & 0 \end{array} \end{array} \right] \left[ \begin{array}{c} I \\ \hline K^{-1}U^T \end{array} \right] \tag{5b}$$

where I is the identity matrix. The relationship between initial and reduced degrees-of-freedom is

$$\left\{ \begin{array}{c} p \\ \hline \Delta \\ \hline H \end{array} \right\} = \left[ \begin{array}{c} I \\ \hline K^{-1}U^T \end{array} \right] \left\{ p \right\} . \tag{6}$$

## UNCOUPLED RESPONSE

Although one of the most important features of the three-dimensional program is the coupled cavity-propellant response, the option of a cavity analysis alone is available to the user. In this case the cavity-solid propellant interface is modeled as an "acoustically hard" boundary. The cavity only option would greatly reduce the solution time and cost and would, in some cases, perhaps suffice. The user need make only two simple adjustments to the input data, and these adjustments are described in the user's guide to the three-dimensional code [16].

## POTENTIAL FLOW CALCULATION

A separate operation is carried out in the sub-routine which performs a potential flow analysis for the purpose of determining the mean flow field in the rocket cavity. As in the case of the eigen-solution, only the smallest repeating geometrical segment need be considered, and, for this calculation, only the cavity portion of the segment with the proper boundary conditions. The same general formulation of the finite element model equations of motion is utilized except that, in this case, the fluid is considered to be incompressible. The mass flow into the cavity from the burning propellant surface is modeled as a cavity-solid propellant interface nodal point quantity. It is calculated by summing the interface surface areas associated with each nodal point lying on the cavity-solid propellant interface. The solution of the resulting set of linear equations for the mean flow velocity components (constant for each cavity tetrahedron) is explained in Reference [11] and will not be discussed here.



(154)

## EVALUATION OF STABILITY INTEGRALS

The final operation consists primarily of the evaluation of the stability integrals associated with the various driving/damping coupling mechanisms which occur in the cavity chamber in the presence of combustion and flow. The stability integrals presently incorporated into the program are those derived in Reference [17] for the three-dimensional case, along with the flow-turning formulation also found in Reference [17]. The use of linear pressure (and therefore constant velocity) tetrahedral elements to represent the cavity region enables an explicit evaluation of the stability integrals, given the acoustic nodal point pressures and element velocities and the mean flow element velocities from the finite element solutions. At present the code does not contain a routine for evaluating nozzle damping or particulate damping. These additional calculations will be added.

The evaluation of stability integrals is for the purpose of calculating the driving/damping coefficient, $\alpha$, a fact well-known to the combustion community. A positive $\alpha$ indicates a stable mode. The net value of $\alpha$ computed by the three-dimensional code is a summation of the computed values of $\alpha_{PC}$ (pressure coupling), $\alpha_{VC}$ (velocity coupling), $\alpha_{FT}$ (flow-turning), and $\alpha_{SD}$ (structural damping). The value of $\alpha_{SD}$ is obtained from the complex eigensolution described in an earlier section; the other three $\alpha$-values are obtained from the evaluation of the stability integrals. It is known that the pressure coupling mechanism always drives the acoustic oscillations, that the velocity coupling mechanism may either drive or damp the oscillations, and that the flow-turning mechanism always damps the oscillations. Response factors [18,19] are input into the program as multiples of the stability integrals for the calculation of the $\alpha$'s obtained from the different coupling mechanisms. These propellant grain-dependent response functions are obtained from other analyses and utilized as direct input into the three-dimensional program.

## COMPARISON WITH ANALYTICAL SOLUTIONS AND EXPERIMENTAL OBSERVATIONS

In order to affirm the accuracy and usefulness of any numerical analysis package it is necessary to make comparisons of results obtained numerically with available analytical closed-form solutions and experimentally obtained results. In the case of a complex analysis procedure such as that of combustion instability, available bases of comparison are limited in both regards. The following results are presented to support the contention of accuracy and utility of the developed package.



(155)

Analytical Comparisons. A right circular cylindrical cavity 254mm long and 254mm in diameter was modeled using an 18° repeating segment consisting of 32 quasi-hexahedral elements, 4 in the radial direction and 8 in the longitudinal direction. Acoustic frequencies corresponding to the first and second logitudinal modes (1L and 2L), the first tangential mode (1T), the first tangential-first longitudinal mode (1T-1L), and the first radial mode (1R) were solved for and are compared with the corresponding analytically obtained frequencies of the cavity. The values are shown in Table 1.

TABLE 1. NUMERICALLY AND ANALYTICALLY CALCULATED ACOUSTIC FREQUENCIES FOR CYLINDRICAL CAVITY

| Mode | Frequency (Hz) | |
|---|---|---|
| | Analytical Solution | Finite Element Solution |
| 1L | 2000 | 1988 |
| 2L | 4000 | 4042 |
| 1T | 2400 | 2378 |
| 1T-1L | 3124 | 3151 |
| 1R | 4994 | 5033 |

As described earlier, a separate potential flow calculation is made in the combustion instability analysis package for the purpose of evaluating the stability integrals. A comparison of the finite element potential flow solution with the analytical solution for the cylindrical cavity is shown in Figure 3.

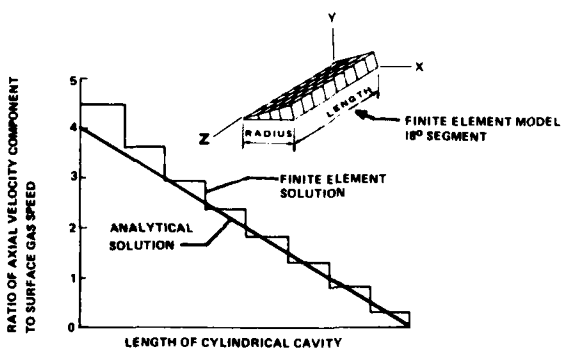


Figure 3. Comparison of finite element and analytical potential flow field solutions for a circular cylinder.

The accuracy of the finite element frequency calculations is seen in Table 1. These results are highly favorable, especially when considering the relatively small number of elements used to model the cavity. The somewhat less satisfying agreement in the case of the finite element potential flow solution can be attributed to the relatively small number of elements, especially near the exhaust end of the cavity where the axial velocity component has its largest value. Additional comparisons with closed-form solutions of the same type have yielded results similar to those cited here.

Experimental Comparisons. The experimental data used for comparison purposes were obtained from Hercules, Inc., Allegany Ballistics Laboratory (ABL) in Cumberland Maryland and result from testing of an early experimental model of the Smokeless CHAPARRAL Motor Assembly, conducted in early 1977. The finocyl geometry of the pulsed motor and the finite element model consisted of a small diameter-to-length ratio cylindrical cavity having four radial slots over approximately one-third of the cavity length. Experimental longitudinal mode frequency and stability data can be compared to corresponding finite element analysis results in Table 2. The test data and numerical results found in Table 2 correspond to a burn distance of 8.03mm. The finite element analyses were performed on the CDC 6600 computer at Redstone Arsenal. The lack of close agreement observed when comparing corresponding net $\alpha$-values can to some extent be attributed to the use of somewhat inaccurate values of response factors, which are presently considered in the program as properties of the propellant, but which are also flow-dependent. However, the qualitatively good agreement between corresponding values can be observed.

TABLE 2. SMOKELESS CHAPARRAL DATA AND FINITE ELEMENT ANALYSIS RESULTS

| Test Data | | Finite Element Analysis | |
|---|---|---|---|
| Frequency (Hz) | $\alpha$ ($sec^{-1}$) | Frequency (Hz) | $\alpha$ ($sec^{-1}$) |
| 323 | -94 | | |
| 290 | -41 | 307 | -198 |
| 644 | -266 | | |
| 640 | -290 | 593 | -220 |
| 909 | -192 | | |
| 927 | -145 | 909 | -148 |



137

The results from additional finite element analyses of the early experimental model of the Smokeless CHAPARRAL Motor Assembly are shown in Table 3. The most notable aspect of this set of finite element analysis results is the prediction of instability in some of the tangential modes (positive values of $\alpha$). This compares quite favorably with ABL tests of the same assembly, which exhibited clear instabilities in tangential modes. Also, ABL test results showed 5-6 separate tangential modes evident in the frequency range of 9000-20,000 Hz.

TABLE 3. HIGHER ACOUSTIC MODE FINITE ELEMENT ANALYSIS RESULTS FOR SMOKELESS CHAPARRAL MOTOR

| Harmonic | Mode | Frequency (Hz) | $\alpha$ ($sec^{-1}$) |
|---|---|---|---|
| K (=1) | 1 | 7992 | -147 |
| | 2 | 13,476 | + 33 |
| | 3 | 15,303 | - 55 |
| | 4 | 15,915 | + 46 |
| | 5 | 17,907 | - 92 |
| N/2 (=2) | 1 | 8981 | -232 |
| | 2 | 15,948 | +162 |
| | 3 | 20,516 | -119 |
| | 4 | 23,693 | - 62 |
| | 5 | 25,644 | - 85 |

The comparisons between numerical and experimental results, which can be made from Tables 2 and 3, would appear to support the contention that the developed finite element package can be of valuable use in predicting the instability of solid rocket systems.

## CONCLUSIONS

The developed computer package performs a linear analysis of the irrotational motions of an inviscid, compressible fluid coupled to the motions of a nearly incompressible, linearly viscoelastic solid, performs a linear potential flow analysis of the irrotational motions of an inviscid, incompressible fluid, and then determines the effect of the flow field and of combustion on the calculated acoustic oscillations. There are obvious limitations attached to any code which is as basic as the restrictions listed above dictate, but it is felt that the developed code presented herein is probably as sophisticated as the present state-of-the-art warrants. It is viewed as having much potential as both a design and a research tool. As the state-of-the-art in combustion technology advances, it is felt that the code can be relatively easily revised and updated to include the new technology; at least it was designed with that provision in mind.

One of the most attractive features of the code is the ease of use. Other extremely important attributes are the fact that it is three-dimensional, that it performs a coupled cavity-solid propellant analysis (or, alternatively, a cavity-only analysis), and that all analyses are automatically linked. Features of the code which do not enhance its reputation also exist, and they too should be pointed out. It is a large program requiring a large amount of storage and it may require long run times, as is the case with any three-dimensional finite element program. Presently, the entire program is in-core computation, but this will, in all probability, be modified. The eigenvalue routine used in the analysis may not be the most efficient one available. This possibility is currently being investigated, and if a more efficient routine can be found, it will be used in place of the one presently employed. In certain instances a two-dimensional (axisymmetric) uncoupled analysis provides sufficient accuracy, and for such cases use of the three-dimensional code might not have merit.

It is felt that the demonstrated attributes of the three-dimensional code far outweigh any foreseen disadvantages, and that it can provide the means of performing important, and heretofore impossible, analyses.

## REFERENCES


1. Standardized Stability Prediction Method for Solid Rocket Motors, Vol. II (Multidimensional Computer Program Users Manual, by D. P. Dudley and R. D. Waugh) and Vol. III (Axial Mode Computer Program Users Manual, by R. L. Lovine and R. C. Waugh), Aerojet Propulsion Company, Sacramento, California, February 1976.
2. Herting, D. N., "Application Manual for NASTRAN Acoustic Cavity Analysis," The MacNeal-Schwendler Corporation, Report MS 116-2, May 1971.
3. Herting, D. N., J. A. Joseph, L. R. Kuusinen and R. H. MacNeal, "Acoustic Analysis of Solid Rocket Motor Cavities by a Finite Element Method," The MacNeal-Schwendler Corporation, Report MS 116-3.
4. NASTRAN Cyclic Symmetry Capability User's Guide, The MacNeal-Schwendler Corporation, EC-180, July 1972.
5. Analysis of a Solid Rocket Motor Cavity, The MacNeal-Schwendler Corporation, Report MS 200, November 22, 1972.
6. Zienkiewicz, O. C., The Finite Element Method in Engineering Science, McGraw-Hill, London, 1971.




157

7. Hackett, R. M., "A Coupled Interior Ballistics Finite Element Combustion Instability Analysis Procedure," Technical Report T-78-72, US Army Missile Research and Development Command, Redstone Arsenal, Alabama, July 1978.
8. Hackett, R. M., "A Coupled Interior Ballistics Finite Element Combustion Instability Analysis Procedure - Part II," Technical Report T-79-68, US Army Missile Command, Redstone Arsenal, Alabama, June 1979.
9. MacNeal, R. H., R. H. Harder and J. B. Mason, "NASTRAN Cyclic Symmetry Capability," TM X-2893 NASTRAN: Users' Experiences, NASA, September 1973, pp. 395-421.
10. Hackett, R. M., "Three-Dimensional Acoustic Analysis of Solid Rocket Motor Cavities," Technical Report RK-76-7, US Army Missile Command, Redstone Arsenal, Alabama, November 1975.
11. Hackett, R. M., "Three-Dimensional Finite Element Acoustic Analysis of Solid Rocket Motor Cavities," Journal of Spacecraft and Rockets, v 13, n 10, October 1976, pp. 585-588.
12. Hackett, R. M., and R. S. Juruf, "Three-Dimensional Finite Element Analysis of Acoustic Instability of Solid Propellant Rocket Motors," Proceedings of the 13th Annual Meeting of the Society of Engineering Science, Inc., Hampton, Virginia, November 1976, pp. 1641-1651.
13. Hughes, T. J. R. and H. Allik, "Finite Elements for Compressible and Incompressible Continua," Proceedings of the Symposium on Application of Finite Element Methods in Civil Engineering, Vanderbilt University, Nashville, Tennessee, November 1969, pp. 27-62.
14. Herrmann, L. R., "Elasticity Equations for Incompressible and Nearly Incompressible Materials by a Variational Theorem," Journal of the American Institute of Aeronautics and Astronautics, v 3, n 10, October 1965, pp. 1896-1900.
15. Cook, R. D., Concepts and Applications of Finite Element Analysis, John Wiley & Sons, Inc., 1974.
16. Hackett, R. M., "User's Manual for FLAP3," Technical Report TK-77-4, US Army Missile Research and Development Command, Redstone Arsenal, Alabama, July 1977.
17. Final Report - T-Burner Testing of Metallized Solid Propellants, Report No. AFRPL-TR-74-28 (F.E.C. Culick - Editor) Air Force Rocket Propulsion Laboratory, Edwards, California, October 1974.
18. Hart, R. W. and F. T. McClure, "Combustion Instability: Acoustic Interaction with a Burning Propellant Surface," Journal of Chemical Physics, v 30, June 1959, pp. 1501-1514.
19. Price, E. W., "Experimental Solid Rocket Combustion Instability," Tenth Symposium (International) on Combustion, The Combustion Institute, 1965, pp. 1067-1082.




167